On the control of optical transmission of aluminosilicate glasses manufactured by the Laser Floating Zone technique

E. Arias-Egido[1], D. Sola[1*], J.A. Pardo[2], J.I. Martínez[3], R. Cases[3], and J.I. Peña[1]

[1]Instituto de Ciencia de Materiales de Aragón, Universidad de Zaragoza-CSIC, Departamento de Ciencia y Tecnología de Materiales y Fluidos, C/ María de Luna 3, 50018 Zaragoza, Spain
[2]Instituto de Nanociencia de Aragón, Universidad de Zaragoza, Departamento de Ciencia y Tecnología de Materiales y Fluidos, C/ María de Luna 3, 50018 Zaragoza, Spain
[3]Departamento de Física de la Materia Condensada, Universidad de Zaragoza, C/ Pedro Cerbuna 12, 50009 Zaragoza, Spain
[*]dsola@unizar.es

Abstract: In this work a detailed study about the properties of aluminosilicate glass rods manufactured by means of the Laser Floating Zone (LFZ) technique is presented. Samples fabrication was carried out in controlled atmosphere using air, nitrogen, and oxygen. Transmission spectra showed that glasses manufactured in oxygen presented high optical transmission in the visible spectral range compared to those manufactured in other environments, thus allowing us to tune their optical behavior between transparent and nearly opaque through the control of the surrounding atmosphere. Microstructure and thermo-mechanical properties were also assessed, showing similar hardness, toughness, flexural strength and glass transition temperature values, and in the same range than other aluminosilicate glasses. Compositional and structural characterization in terms of Energy Dispersive X-ray Spectroscopy (EDX) and Electron Paramagnetic Resonance (EPR) allowed us to determine the origin of optical transmission dependence on the fabrication atmosphere.

OCIS codes: (160.2750) glass and other amorphous materials; (160.6990) transition-metal-doped materials; (300.1030) absorption; (350.3390) laser materials processing.

References and links

1. W. M. Steen, and J. Mazumder, *Laser material processing* (Springer, 2003).
2. D. Bäuerler, *Laser processing and chemistry* (Springer, 2000).
3. M.V. Allmen, and A. Blatter, *Laser-beam interactions with materials: Physical principles and applications* (Springer, 2002).
4. Y. Pauleau, *Materials surface processing by directed energy techniques* (Elsevier Science, 2006).
5. H. Misawa, and S. Juodkazis, *3D laser microfabrication* (Wiley, 2006).
6. G.S. Upadhyaya, *Sintered Metallic and Ceramic Materials: Preparation, Properties and Applications* (Wiley, 1999).
7. E.A. Olevsky, and R. Bordia, *Advances in Sintering Science and Technology* (Wiley, 2010).
8. D.R. Ardila, M.R.B. Andreeta, S.L. Cuffini, A.C. Hernandes, J.P. Andreeta, and Y.P. Mascarenhas, "Laser heated pedestal growth of Sr_2RuO_4 single-crystal fibers from $SrRuO_3$," J. Cryst. Growth **177**(1–2), 52–56 (1997).
9. A.S.S. de Camargo, L.A.O. Nunes, M.R.B. Andreeta, and A.C. Hernandes, "Near-infrared and up-conversion properties of neodymium-doped $RE0.8La_{0.2}VO_4$ (RE = Y, Gd) single-crystal fibers grown by the laser-heated pedestal growth technique," J. Phys. Condens. Matter. **14**(50), 13889–13897 (2002).
10. D. Sola, D. Conejos, J. M. De Mendivil, L. O. SanMartín, G. Lifante, and J.I. Peña, "Directional solidification, thermo-mechanical and optical properties of $(Mg_xCa1_{-x})_3Al_2Si_3O_{12}$ glasses doped with Nd^{3+} ions," Opt. Express **20**, 26356-26358 (2015).

11. D. Sola, R. Balda, J.I. Peña, and J. Fernandez, "Site-selective laser spectroscopy of Nd^{3+} ions in $0.8CaSiO_3$-$0.2Ca_3(PO_4)_2$ biocompatible eutectic glass-ceramics," Opt. Express **20**, 10701-10711 (2012).
12. D. Sola, and J.I. Peña, "Laser machining of Al_2O_3-ZrO_2 ($3\%Y_2O_3$) eutectic composite," J. Eur. Ceram. Soc. **32**, 807-814 (2012).
13. J. Llorca, and V.M. Orera, "Directionally-solidified eutectic ceramic oxides," Prog. Mater. Sci. **51**, 711-809 (2006).
14. D. Sola, F.J. Ester, P.B. Oliete, and J.I. Peña, "Study of the stability of the molten zone and the stresses induced during the growth of Al_2O_3-$Y_3Al_5O_{12}$ eutectic composite by the laser floating zone technique," J. Eur. Ceram. Soc. **31**, 1211-1218 (2011).
15. F.J. Ester, D. Sola, and J.I. Peña, "Thermal stresses in the Al_2O_3-$ZrO_2(Y_2O_3)$ eutectic composite during the growth by the laser floating zone technique," Bol. Soc. Esp. Ceram. **47**, 352-357 (2008).
16. J. Kohli, and J.E. Shelby, "Rare-earth Aluminosilicate Glasses," J. Am. Ceram. Soc. **73**, 39-42 (1990).
17. M. J. Hyatt, and D. E. Day, "Glass properties in the yttria-alumina-silica system," J. Am. Ceram. Soc. **70**, 283-287 (1987).
18. P. Vomacka, and O. Babushkin, "Yttria-alumina –silica glasses with addition of zirconia," J. Eur. Ceram. Soc. **15**, 921-928 (1995).
19. S.L. Lin, and C.S. Hwang, "Structures of CeO_2-Al_2O_3-SiO_2 glasses," J. Non-Cryst. Solids **202**, 61-67 (1996).
20. E.M. Erbe, and D.E. Day, "Properties of Sm_2O_3-Al_2O_3-SiO_2 glasses for in vivo applications" J. Am. Ceram. Soc. **73**, 2708-2713 (1990).
21. M.A. Sainz, M.I. Osendi, and P. Miranzo, "Protective Si–Al–O–Y glass coatings on stainless steel in situ prepared by combustion flame spraying," Surf. Coat. Technol. **202**, 1712-1717 (2008).
22. K. Nassau, *The physics and chemistry of color. The fifteen causes of color* (Wiley, 2001).
23. ASTM C1327-99, *Standard Test Method for Vickers Indentation Hardness of Advanced Ceramics* (1999).
24. G. Fargas Ribas, D. Casellas Padró, L.M. Llanes Pitarch, and M. Anglada Gomilla, "Thermal shock resistance of Y-TZP with Palmqvist craks," Bol. Soc. Esp. Ceram. **42**(1), 9-14 (2003).
25. S. Takahashi, D. R. Neuville, H. Takebe, "Thermal properties, density and structure of percalcic and peraluminus CaO–Al_2O_3–SiO_2 glasses," J. Non-Cryst. Solids **411**, 5–12 (2015).
26. R.J. Hand, and D.R. Tadjiev, "Mechanical properties of silicate glasses as a function of composition," J. Non-Cryst. Solids **356**, 2417–2423 (2010).
27. F.S. Shirazi, M. Mehrali, A.A. Oshkour, H.S.C. Metselaar, N.A. Kadri, and N.A. Abu Osman, "Mechanical and physical properties of calcium silicate/alumina composite for biomedical engineering applications," J. Pharm. Biomed. Anal. **30**, 168–175 (2014).
28. SCHOTT CERAN® Ceran Suprema® Cooktop Panels, Technical Delivery Specification TL 1 00 03 01 – 00.
29. N.P. Bansal, and R.H. Doremus, *Handbook of Glass Properties* (Academic Press Handbook Series, 1986).
30. N. Shimoji, T. Hashimoto, H. Nasu, and K. Kamiya, "Non-linear optical properties of Li_2O–TiO_2–P_2O_5 glasses", J. Non-Cryst. Solids **324**, 50–57 (2003).
31. A. Shaim, and M. Et-tabirou, "Role of titanium in sodium titanophosphate glasses and a model of structural units" Mater. Chem. Phys. **80**, 63–67 (2003).
32. C.R. Bamford, *Colour Generation and Control in Glass* (Elsevier, 1977).
33. M. Farouk "Effect of TiO_2 on the structural, thermal and optical properties of BaO–Li_2O–diborate glasses," J. Non-Cryst. Solids **402**, 74–78 (2014).

1. Introduction

Laser technology has been employed for several years in the processing of different materials [1,2]. Among the key characteristics that make laser radiation such an attractive tool for this purpose, noteworthy are coherence, monochromaticity, polarization and collimation, which allow adjusting power distribution with conventional optical elements as well as placing the processing source outside reaction chambers. Additionally, both high energy and power densities can be achieved so that focused laser radiation provides a non-contact micron-sized tool to be used for localized material processing which allows adjacent areas remain unchanged. Among laser processing techniques, it is worth mentioning surface treatments, welding, cutting, drilling, machining [1-5], ceramic oxide sintering [6,7], and directional solidification applied to the growth of single crystals, glasses, glass-ceramics or production of aligned eutectics [8-13].

There are currently several directional solidification techniques for obtaining advanced ceramic materials. Among them, it is worth highlighting the laser floating zone (LFZ) in which the heat source is provided by an infrared laser. The main advantages of this technique

are the possibility of growing materials with very high melting points and the control of the resulting microstructure by means of solidification rates, which allow obtaining materials with very small phase size or even glasses [10-15]. In addition, this technique permits the possibility to displace, rotate and counter-rotate at different speeds allowing the thickening and the thinning of the grown rod and favoring a homogeneous distribution of the temperature in the molten zone. Thus, phase size can be controlled and hence its mechanical properties [13]. Finally, as the growth takes place in a sealed chamber it is possible to work in different atmospheres.

Rare-earth aluminate and aluminosilicate glasses have been of great interest for many years due to their high elastic modulus and hardness, high refraction index, excellent optical properties, and good corrosion resistance [16-21].

In this work we have studied how to control the optical transmittance in aluminosilicate glasses manufactured by means of the LFZ technique. Surrounding medium, in terms of oxidizing or reducing atmosphere, has resulted the figure of merit to modify the oxidation state of some paramagnetic elements contained in the glass, which in turn, has led to optical transmission modification. Microstructural, thermal, mechanical, and optical properties of resulting glasses have been assessed as a first step with the future purpose of using these glasses as host matrices of trivalent rare-earth ions, such as Nd^{3+} and Er^{3+}, for optical applications such as optical amplifiers or lasers, or for functional purposes such as the fabrication of micron-sized optical windows in the visible range.

2. Experimental

2.1 Sample fabrication

Glass samples were obtained departing from a commercial glass-ceramic, Ceran Suprema®, manufactured by Schott. Parallelepiped-shaped slices of about 50×2×2 mm^3 (length × width × height) were cut from the bulk glass-ceramic by using a slow speed saw (Accutom-5, Struers) and processed by means of the LFZ technique to obtain glass rods.

The LFZ system includes a CO_2 laser of 600 W (Electronic Engineering Blade 600) emitting in 10.6 μm wavelength and an in-house built growth chamber with gold-coated metal mirrors for the beam focusing and two vertical axes for the sample displacement [13]. Both axes have independent rotation and translation movement. The mirror system inside the chamber consists of a reflaxicon that transforms the solid beam into a ring that is deflected by a flat mirror at 45º and focused in the ceramic rod by a parabolic mirror producing homogenous heating. Placed the precursor in the upper axis, the growth process starts heating its lower end. Once a drop is formed, a small seed placed in the lower axis is approached until a liquid bridge between the precursor and the seed is established. The seed is then moved away at the same time as the precursor is moved towards the molten zone, maintaining constant the volume of the liquid zone. To increase or decrease the rod diameter, the growth rate can be lower or higher respectively than the precursor speed. The precursor and the grown rod are counter-rotated to improve the heat distribution in the molten zone. This technique permits the control of the solidification rate, providing high axial and radial thermal gradients at the liquid-solid interface, of paramount importance in the microstructure control, and opens up the possibility of fabricating glasses, glass-ceramics and single crystals [14, 15].

In particular in this case, in order to obtain bubble-free glasses, precursor and rod growth rates were fixed at 100 and 300 mm/h respectively. Finally, the growth chamber allowed working in different atmospheres, namely: air, nitrogen and oxygen, applying a bit of overpressure inside the chamber to ensure that any leaks were outwards.

2.2 Characterization techniques

Composition of glasses was determined by means of Field Emission Scanning Electron Microscopy (FESEM) using a Carl Zeiss MERLIN microscope with Energy Dispersive X-ray

detector (EDX). The amorphous character of glass samples was analyzed by X-ray Diffraction (XRD) using a Bruker D8 Advance diffractometer.

Paramagnetic species in the glass were determined by continuous wave Electronic Paramagnetic Resonance (EPR) measurements using a Bruker ELEXIS E-580 spectrometer working at either X- (microwave frequencies ~ 9.5 GHz) or Q- (microwave frequencies ~ 34 GHz) bands. Experiments were taken at 80 K and room temperature, with identical results.

Differential Scanning Calorimetry (DSC) analyses were carried out in order to determine recrystallization and glass transition temperatures using a SDT Q600 V8.3 Build 101 machine in an air atmosphere from room temperature to 1200 ºC at a rate of 10 ºC/min.

Mechanical characterization was carried out by a micro-hardness tester Matsuzawa MXT-70, a nano-indenter Agilent Technologies G200 and a universal testing machine Instron 5565.

Optical transmission spectra were obtained by means of a Hitachi U-3400 spectrophotometer.

3. Results and discussion

3.1. Optical characterization

It was observed that the nature of the surrounding atmosphere in which glasses were grown had a great influence on the resulting samples. Figs. 1(a), (b) and (c) show samples grown in air, nitrogen and oxygen respectively. Depending on the oxidizing or reducing characteristics of the surrounding atmosphere, light transmission changed so that the higher the oxidizing character of the atmosphere, the higher the optical transmittance in the visible range. In fact, the glass grown in oxygen was colorless to the naked eye.

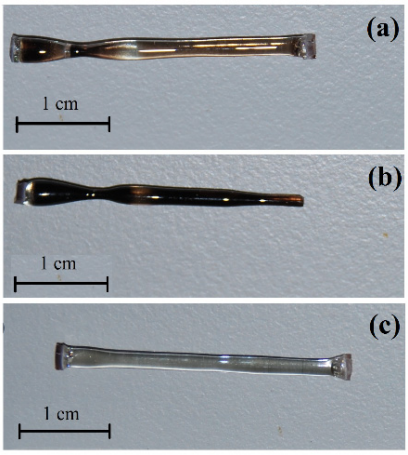

Fig. 1. Optical photographs showing the samples grown in different atmospheres: (a) air, (b) nitrogen, (c) oxygen.

Fig. 2 shows room temperature transmission spectra in the 300-800 nm wavelength range for these three samples and, for comparison purposes, the transmission spectrum of departing glass-ceramic is also presented. The sample grown in oxygen presented the highest transmittance in the visible range, in agreement with its colorless and transparent aspect. For instance, at 500 nm the oxygen-grown glass sample had an optical transmittance around 81%, whereas air-grown and nitrogen-grown glass transmittance was around 35 and 11% respectively. Departing glass-ceramic optical transmittance at this wavelength was around 14%. Thus, oxidizing or reducing atmosphere can be used to control and modify optical transmission.

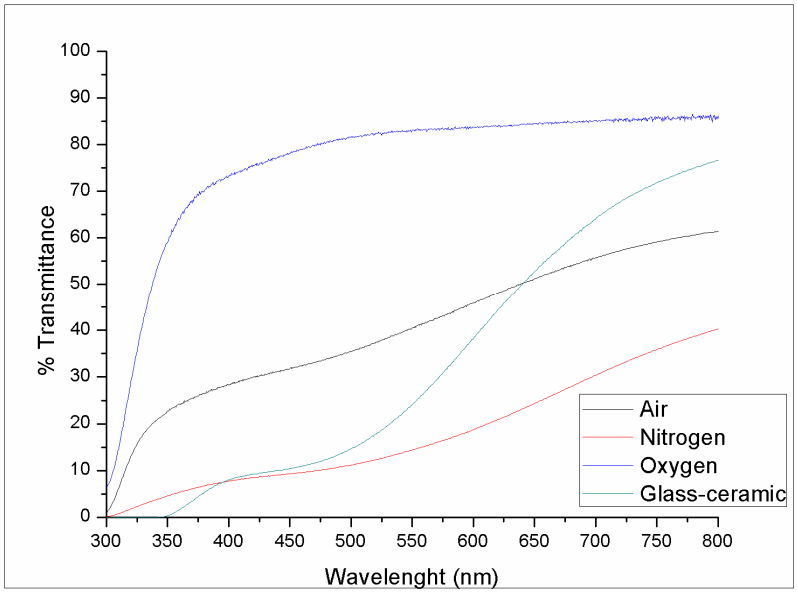

Fig. 2. Visible range transmission spectra of glasses grown in different atmospheres and departing glass-ceramic.

3.2. Compositional and microstructural characterization

Compositional and microstructural characterization was carried out aiming to determine the origin of optical transmission modification. Firstly, the amorphous character of glass samples was confirmed by XRD. Secondly, semi-quantitative compositional analyses were carried out by EDX microanalysis to ascertain the main elements of the samples. Table 1 shows that both glass-ceramic and glasses were composed of SiO_2 and Al_2O_3 as majority components with small amounts (lower than 2% atomic) of NaO, MgO, TiO_2, ZnO and ZrO_2.

Table 1. Results of the EDX analyses of the glasses grown in different atmospheres measured in at.%

Element	Departing glass-ceramic	Air	Oxygen	Nitrogen
Na	1.36	0.88	0.89	1.05
Mg	1.56	1.70	1.57	1.60
Al	24.63	27.78	25.54	25.62
Si	68.65	66.51	68.95	68.23
Ti	1.79	1.92	1.80	1.80
Zn	1.20	0.33	0.43	0.85
Zr	0.81	0.88	0.82	0.85

It can be observed that the composition was almost the same for the three glass samples regardless of the atmosphere in which they were grown. However, by comparing their composition with that of the departing glass-ceramic, a loss of NaO and ZnO has taken place. In either case this is not responsible for the optical transmission modification since the same

compositional variations were produced in the three glass samples as far as NaO is concerned, and there is no apparent correlation between the amount of ZnO and the color of the glasses. On the other hand, it is well known that small amounts of transition metal ions are often used for coloring glasses [22]. In this way, optical transmission variation might be attributed to TiO_2 or ZnO which are part of glass composition as minority components.

In order to prove it, EPR analyses were conducted on the three samples. Fig. 3(a) shows the EPR spectrum at X band (microwave frequency ~ 9.5 GHz) of a glass grown in oxygen. Two characteristic features can be identified: at a field position around 160 mT a single, slightly asymmetric signal is detected. It can be described by means of a Spin Hamiltonian H containing just a Zeeman interaction:

$$H = \mu_B \vec{B} \tilde{g} \vec{S} \tag{1}$$

where μ_B is the Bohr magneton, $\vec{B}$ is the magnetic field vector, $\tilde{g}$ is the gyromagnetic tensor and $\vec{S}$ is the electronic spin vector (S = 1/2). Its position (g_{eff} = 4.3) and shape is typical of Fe^{3+} centers in a low symmetry environment. Besides, a group of signals in the 280 mT - 420 mT region is seen. Those signals can be described by means of a Spin Hamiltonian containing Zeeman and hyperfine interactions:

$$H = \mu_B \vec{B} \tilde{g} \vec{S} + \vec{S} \tilde{A} \vec{I} \tag{2}$$

where $\tilde{A}$ is the hyperfine tensor and $\vec{I}$ is the nuclear spin (I = 7/2). This value for the nuclear spin, as well as the values of the principal values of both gyromagnetic and hyperfine tensors ($g_1 = g_2 = g_\perp = 1.99$, $g_3 = g_\parallel = 1.94$, $A_1 = A_2 = A_\perp = 190$ MHz, $A_3 = A_\parallel = 510$ MHz) allow identifying this signal as due to a V^{4+} species. No other paramagnetic centers are detected.

It could seem surprising that EPR measurements revealed the presence of transition metals not detected in the compositional analysis. This is due to the high sensitivity of that spectroscopic signal since it is able to detect very low concentration of paramagnetic centers. In this case, we can suppose that Fe^{3+} and V^{4+} centers appeared in the glass samples with abundance far lower than 1%, and consequently were not detected by the EDX microanalysis.

EPR spectrum at X band (microwave frequency ~ 9.5 GHz) of glass grown in nitrogen is seen in Fig. 3(b). No evidence of Fe^{3+} or V^{4+} centers is detected. Only one signal at a field position ~ 350 mT appeared. It can be described by means of a Spin Hamiltonian similar to equation (1), with a nearly isotropic Zeeman interaction. When the same sample was measured at Q band (microwave frequency ~ 34 GHz, not shown) the signal revealed differences between the g tensor principal values:

$$g_1 = 1.93,\ g_2 = 1.95,\ g_3 = 1.98 \tag{3}$$

These values are typical of Ti^{3+} centers. Last, EPR spectrum of glass grown in air, Fig. 3(c), showed traces of the three previously described features (Fe^{3+}, V^{4+} and Ti^{3+} centers). In all the cases with a lower intensity if compared to the signals detected in glasses grown in oxygen and in nitrogen.

Although signal in Fig. 3(b) cannot in principle be assigned univocally to Ti^{3+} centers, such assignment is very likely since, besides the obtained gyromagnetic principal values are compatible, it allowed developing a comprehensive model fully coherent with all the experimental evidence, as we will describe later in Section 3.4.

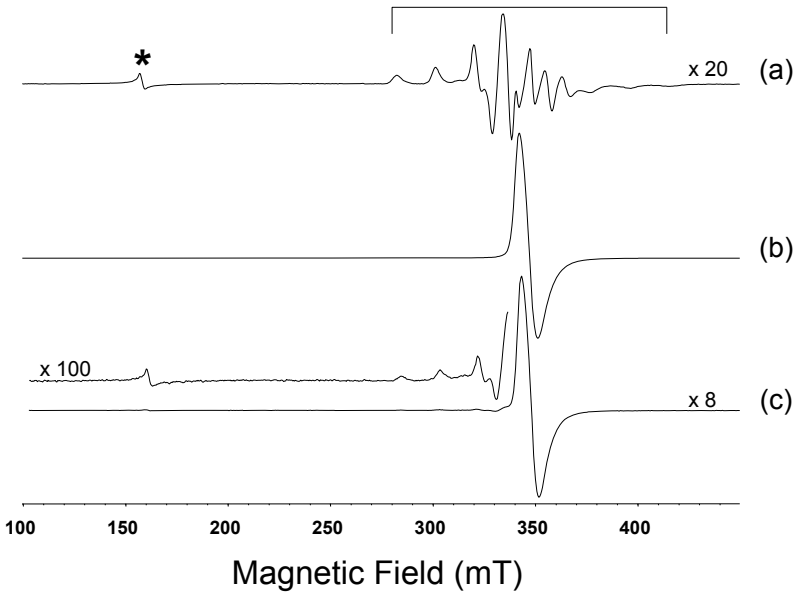

Fig. 3. EPR spectra measured in the glasses grown in different atmospheres: (a) oxygen, (b) nitrogen, (c) air. A star and an open box mark the signals related to Fe^{3+} and V^{4+} centers in Fig. 3(a) (see text). The signal in Fig. 3(b) is assigned to Ti^{3+} centers (see text). In order to make the differences in intensity of the signals between the spectra visible, the enlargement of the spectra with respect to Fig. 3(b) are indicated. The enlarged detail of Fig. 3(c) allows seeing the presence of the Fe^{3+} and V^{4+} signals beside the Ti^{3+} one.

3.3. Thermo-mechanical characterization

DSC analyses were performed on the samples reporting glass transition temperatures, Tg, at 900 ºC approximately, and peak crystallization temperatures, Tc, about 1050 ºC for the three samples.

Table 2 presents the mechanical properties for the three glass samples, assessed in terms of Vickers hardness (HV), toughness (K_{IC}), and flexural strength. Furthermore, Young´s modulus was determined from nano-indentation tests. Vickers hardness tests performed in the three glasses showed hardness values ranging between 5.21 and 5.33 GPa. Worth of mention is the fact that the obtained glass-ceramic hardness is higher, specifically 6.44 GPa, due to the presence of the crystalline phase contained in the glass-ceramic. Toughness was evaluated indirectly by indentation method making direct measurements of crack lengths created by the diamond indenter during hardness test [23]. Recorded values for the glass samples were between 1.37 and 1.44 MPa $m^{1/2}$. In this case glass-ceramic toughness was in the same range as the glass samples. Nano-indentation tests reported Young´s modulus between 73.6 and 83.4 GPa for the three glass samples and 87.8 GPa for the glass-ceramic. The latter is higher than the former for the same reason as in the case of hardness.

Table 2 also shows the results of the three-point flexure test, revealing values of the flexural strength between 402 and 606 MPa for the glasses. In the case of the departing glass-ceramic, an average value of 104 MPa was obtained. This difference may be due to the presence of residual stresses inside the glasses since samples were not annealed after the growing process [24]. The high dispersion is due to the difficulty of growing flaw-free glasses, which was confirmed by means of the Weibull statistical study, obtaining low m values between 2.80 and 4.13, which indicates a wide range of flaw sizes.

Taking into account all the above, it can be said that thermo-mechanical properties in the typical range for aluminosilicate glasses have been obtained [25-29].

Table 2. Mechanical properties of the glasses grown in different atmospheres and the initial glass-ceramic.

	Young modulus (GPa)		Hardness (GPa)		K_{IC} (MPa $m^{1/2}$)		Flexural strength (MPa)	
	Mean	**Std. Dev.**	**Mean**	**Std. Dev.**	**Mean**	**Std. Dev.**	**Mean**	**Std. Dev.**
Glass-ceramic	87.8	1.0	6.44	0.18	1.24	0.04	104	24
Air	83.4	1.2	5.21	0.12	1.44	0.08	606	122
Oxygen	73.6	0.7	5.24	0.25	1.37	0.02	402	149
Nitrogen	80.1	1.7	5.33	0.11	1.48	0.04	564	145

3.4 Descriptive model

The obtained experimental evidence can be understood on the basis of a model that considers the composition of the glasses as well as their chemical and physical properties.

When a multicomponent glass is prepared by rapid cooling from high temperatures, a local variability of oxygen concentrations and metal environments may take place, in such a way that, although the most common oxidation state of titanium in glasses is as Ti^{4+} [30,31], a small amount of Ti^{3+} centers can occur. Titanium can exhibit both trivalent and tetravalent valence states in glasses and the ratio of these two species depends on the glass type, composition and condition of melting [22,32]. Depending on the concentration, titanium typically shows tetrahedral and/or octahedral coordination with oxygen. Silicate glasses favor the colorless high tetravalent (Ti^{4+}) ions while phosphate glasses initiate the presence of purple trivalent (Ti^{3+}) ions [33]. By comparing the intensity of the Ti^{3+} EPR signal in Figs. 3(b) and 3(c) with those of Fe^{3+} and V^{4+} signals in Figs. 3(a) and 3(c), the Ti^{3+} centers concentration could be inferred to be around 1‰ or lower. Additionally, comparison of the line width of the EPR signals indicates that Ti^{3+} entities are not clustering in the glasses but they are dispersed, as broadening because dipole-dipole interactions is small. Despite these small concentrations, Ti^{3+} centers can be responsible for both the optical properties of the departure glass-ceramic material and the glasses grown in nitrogen. When the glass is grown in an oxygen atmosphere, the strong reactive conditions cause the oxidation of the Ti^{3+} centers to Ti^{4+} (non-paramagnetic), as well as that of Fe^{2+} and V^{3+}centres, which are present in the samples as small impurities, to Fe^{3+} and V^{4+}, respectively. Interestingly, EPR spectra demonstrate that all the iron and vanadium centers in glasses grown in nitrogen are all in the EPR-silent forms Fe^{2+} and V^{3+}, and also that the oxygen atmosphere is able to oxidize 100% of the Ti^{3+} centers in the glasses. As far as glasses grown in air are concerned, EPR spectrum shown in Fig. 3(c) indicates that only a partial oxidation took place during growth. Although our measurements do not allow an accurate quantitative comparison, it can be estimated 10%-40% of the centers, and it is larger for the iron centers in comparison with titanium and vanadium ones. Moreover, optical measurements indicate that such glasses keep the dark color. Then we can conclude that only a very oxygen-rich atmosphere is able to verify a complete "clearing" (Ti^{3+} oxidation) process, and that probably some small metal impurities in the sample, as iron, could protect the glass against clearing during the growing process when the atmosphere contains some oxygen.

On the other hand, thermo-mechanical properties are mostly related with the bulk structure, then the oxidation process hardly affect them as all the centers involved are small impurities.

4. Conclusions

It was possible to fabricate glasses in controlled atmospheres departing from glass-ceramics by means of the Laser Floating Zone (LFZ) technique, obtaining compositional and thermo-mechanical characteristics in the expected range for glasses with similar composition.

Optical properties of these glasses have been controlled by changing the atmosphere in which samples were grown, obtaining a colorless glass when prepared in an oxidizing atmosphere and dark glasses when using reducing atmospheres.

By using EPR technique, it was shown that the nitrogen-grown glasses showed a very small amount of Ti^{3+} ions responsible for giving the samples such dark tonality.

Although the most common oxidation state of Titanium inside the glass is as Ti^{4+}, non-oxidizing cooling conditions in this case induced the presence of a small amount of Ti^{3+} centers. If cooling occurs in an oxygen atmosphere, it has a strong oxidizing effect, making Ti^{3+} centers disappear transforming them into Ti^{4+}, leading to the disappearance of the coloring of the glass. Our results point out that both concentration of oxygen in the growing atmosphere and the presence of small transition metal impurities could be used to control optical properties without a change in the thermo-mechanical ones.

Even though more study has to be done in this field, these results prove that the LFZ technique allows tailoring the optical transmission of aluminosilicate glasses during the fabrication process. The control on this optical property may be applied for functional purposes such as the fabrication of micron-sized optical windows in the visible range or in the fabrication of Rare-Earth doped glass matrices for optical amplifiers or lasers.

Acknowledgments

Dr. Daniel Sola thanks the Bosch and Siemens Home Appliances Group for the financial support of his contract. Financial support from University of Zaragoza (project nº UZ2015-CIE-07) and “Grupos de Investigación” program of the Aragon Autonomous Government (ref. B18) is acknowledged by Dr. J.I. Martínez. Mr. Eduardo Arias-Egido thanks the Ministry of Economy and Competitiveness of the State General Administration for the financial support for his Ph.D. studies.